Supporting Information for

^{19}F Dynamic Nuclear Polarization at Fast Magic Angle Spinning for NMR of HIV-1 Capsid Protein Assemblies

Manman Lu[1,2,3,#], Mingzhang Wang[1,2,#], Ivan V. Sergeyev[4,#], Caitlin M. Quinn[1], Jochem Struppe[4], Melanie Rosay[4], Werner Maas[4], Angela M. Gronenborn[2,3*], Tatyana Polenova[1,2*]

[1]Department of Chemistry and Biochemistry, University of Delaware, Newark, Delaware 19716, United States; [2]Pittsburgh Center for HIV Protein Interactions, University of Pittsburgh School of Medicine, 1051 Biomedical Science Tower 3, 3501 Fifth Ave., Pittsburgh, PA 15261, United States; [3]Department of Structural Biology, University of Pittsburgh School of Medicine, 3501 Fifth Ave., Pittsburgh, PA 15261, United States; [4]Bruker Biospin Corporation, 15 Fortune Drive, Billerica, MA, United States

[#]These authors have contributed equally

***Corresponding authors:** Angela M. Gronenborn, Department of Structural Biology, University of Pittsburgh School of Medicine, 3501 Fifth Ave., Pittsburgh, PA 15260, USA, Tel.: (412) 648-9959; Email: amg100@pitt.edu; Tatyana Polenova, Department of Chemistry and Biochemistry, University of Delaware, Newark, DE, USA, Tel.: (302) 831-1968; Email: tpolenov@udel.edu

Keywords: magic angle spinning, ^{19}F NMR, HIV-1 capsid, DNP

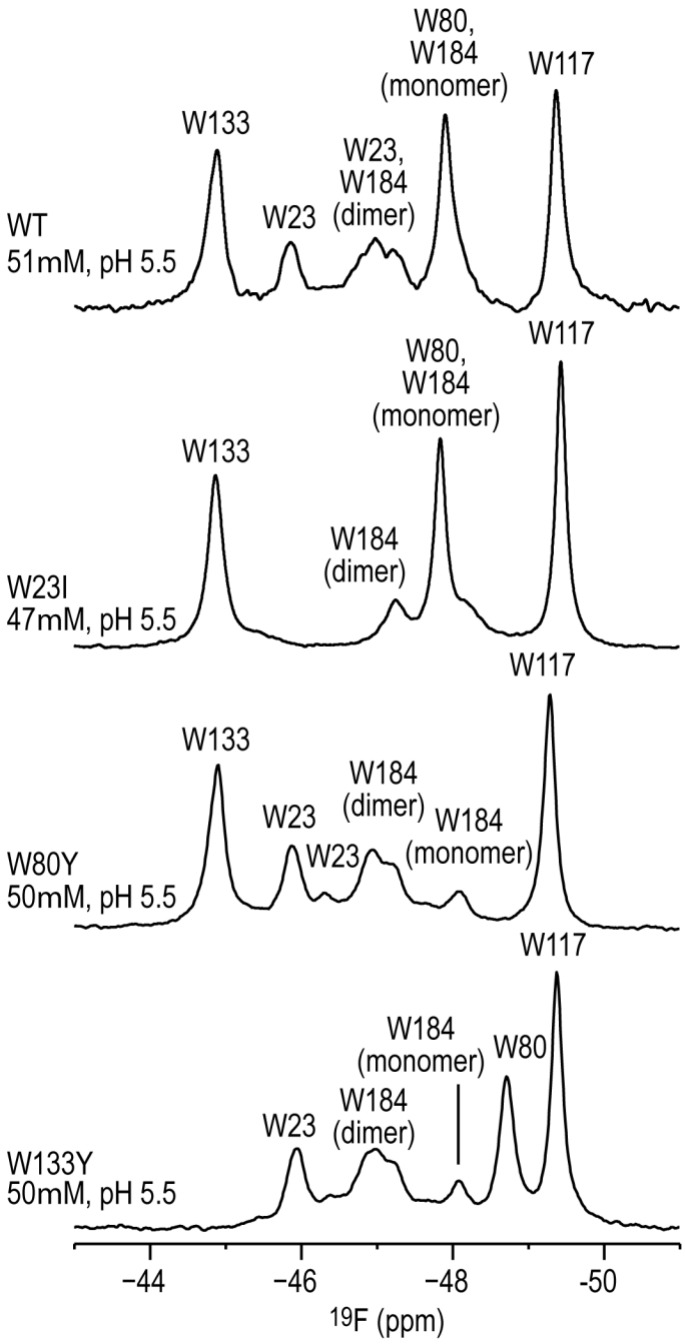

Figure S1. ^{19}F solution NMR spectra of (top to bottom) 5-^{19}F-Trp, U-^{15}N CA (top) and 5-^{19}F-Trp,U-^{15}N CA mutants W23I, W80Y, and W133Y. The spectra were recorded at 14.1 T (564.8 MHz ^{19}F Larmor frequency). The sample conditions are listed next to each spectrum. Assignments are shown on top.

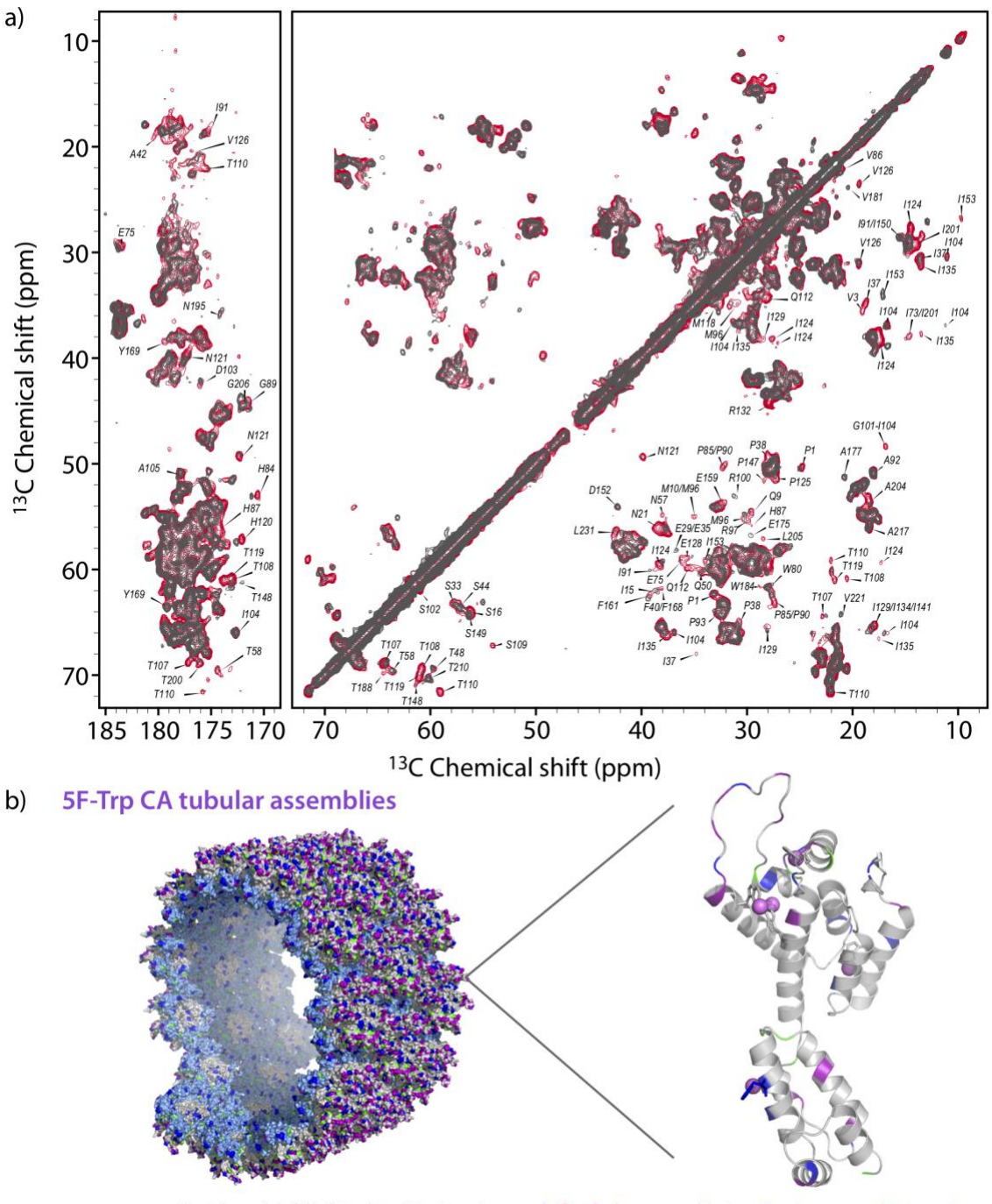

Figure S2. (a) Superposition of ^{13}C-^{13}C RFDR spectra of 5F-Trp, U-^{13}C,^{15}N CA tubular assemblies in the absence (red) and presence of 12 mM AMUPol (grey) at 290 K, 19.96 T (Larmor frequencies 850.4 MHz (^{1}H) and 213.8 MHz (^{13}C)), and 40 kHz MAS. (b) Residues whose resonances are affected by the biradical doping are mapped onto a 3D model of a section of the CA tube (PDBID: 3j4f) and the CA monomer (PDBID: 4XFX). These residues are colored in purple (peak shift), blue (decreased peak intensity), and green (increased peak intensity). The five 5F-Trp residues (W23, W80, W117, W133 and W184) are shown in stick representation, and the fluorine atoms as purple spheres.

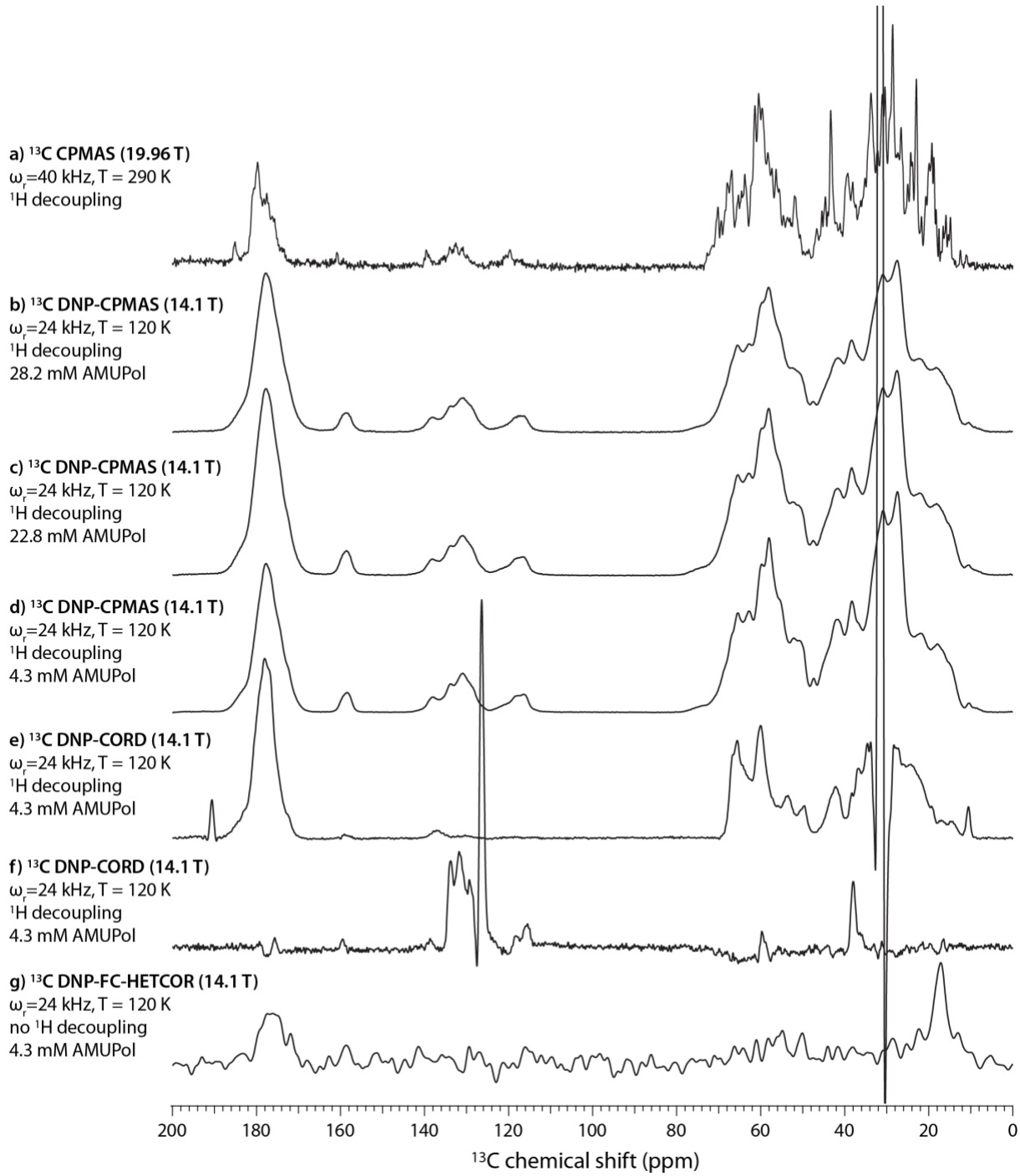

Figure S3. a) 1D ^{13}C CPMAS spectrum of 5F-Trp CA assemblies acquired at 19.96 T, T = 290 K, and MAS frequency of 40 kHz. ^{1}H decoupling was performed with 10 kHz TPPM. b)-d) DNP-enhanced ^{13}C CPMAS spectra of 5F-Trp CA assemblies doped with 28.2, 22.8, and 4.3 mM AMUPol. e)-g) 1D traces extracted from a 2D DNP-enhanced CORD (e,f) and 2D DNP-enhanced ^{19}F-^{13}C HETCOR spectra of 5F-Trp CA assemblies doped with 4.3 mM AMUPol. The spectra shown in b)-g) were acquired at 14.1 T, T = 120 K, and a MAS frequency of 24 kHz. In b)-f), ^{1}H decoupling was performed with 166.7 kHz SPINAL-64. In g), no ^{1}H decoupling was applied.

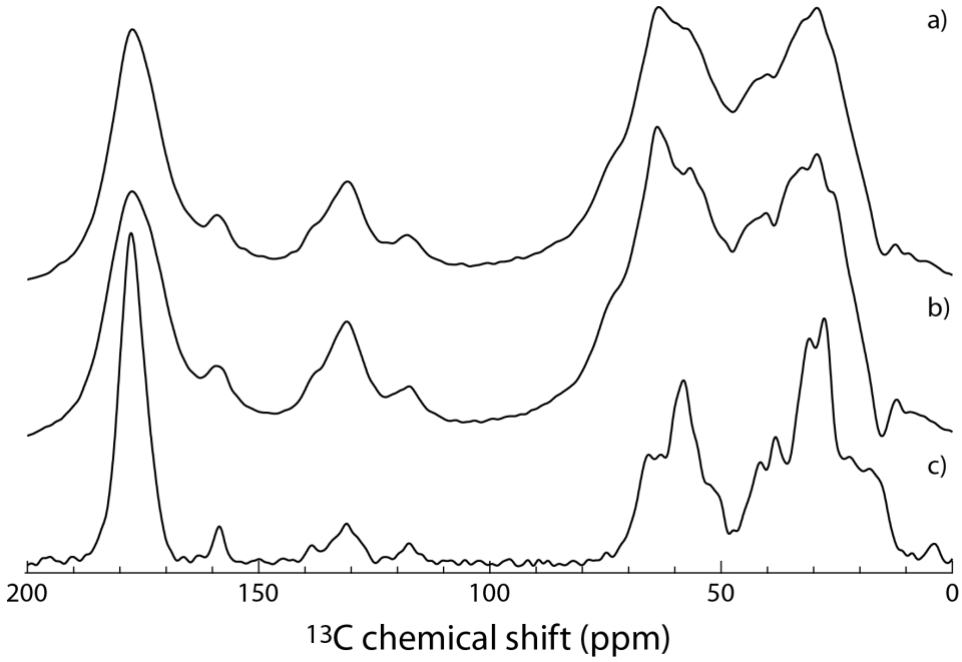

Figure S4. Single-pulse-excitation DNP-enhanced MAS NMR spectra of 5F-Trp CA assemblies doped with a) 28.2 mM AMUPol, b) 22.8 mM AMUPol, and c) 4.3 mM AMUPol. The spectra were acquired with 16 scans at 14.1 T, T = 120 K, microwave power of 13.8 W, and a MAS frequency of 24 kHz. ^{1}H decoupling was performed with 166.7 kHz SPINAL-64.

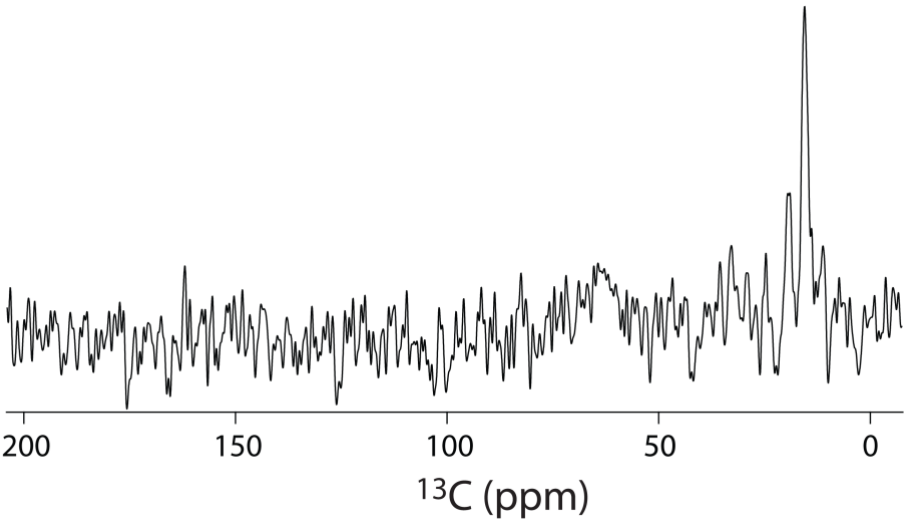

Figure S5. ^{19}F-^{13}C CPMAS NMR spectrum of 5F-Trp A14C/E45C/W184A/M185A CA cross-linked hexamer tubular assemblies at 290 K, 19.96 T (Larmor frequencies 850.4 MHz (^{1}H), 800.1 MHz (^{19}F), and 213.8 MHz (^{13}C)), and 40 kHz MAS. The spectrum was acquired with 43,008 scans, total experiment time was 24 hours. 10 kHz ^{1}H decoupling was applied during acquisition.

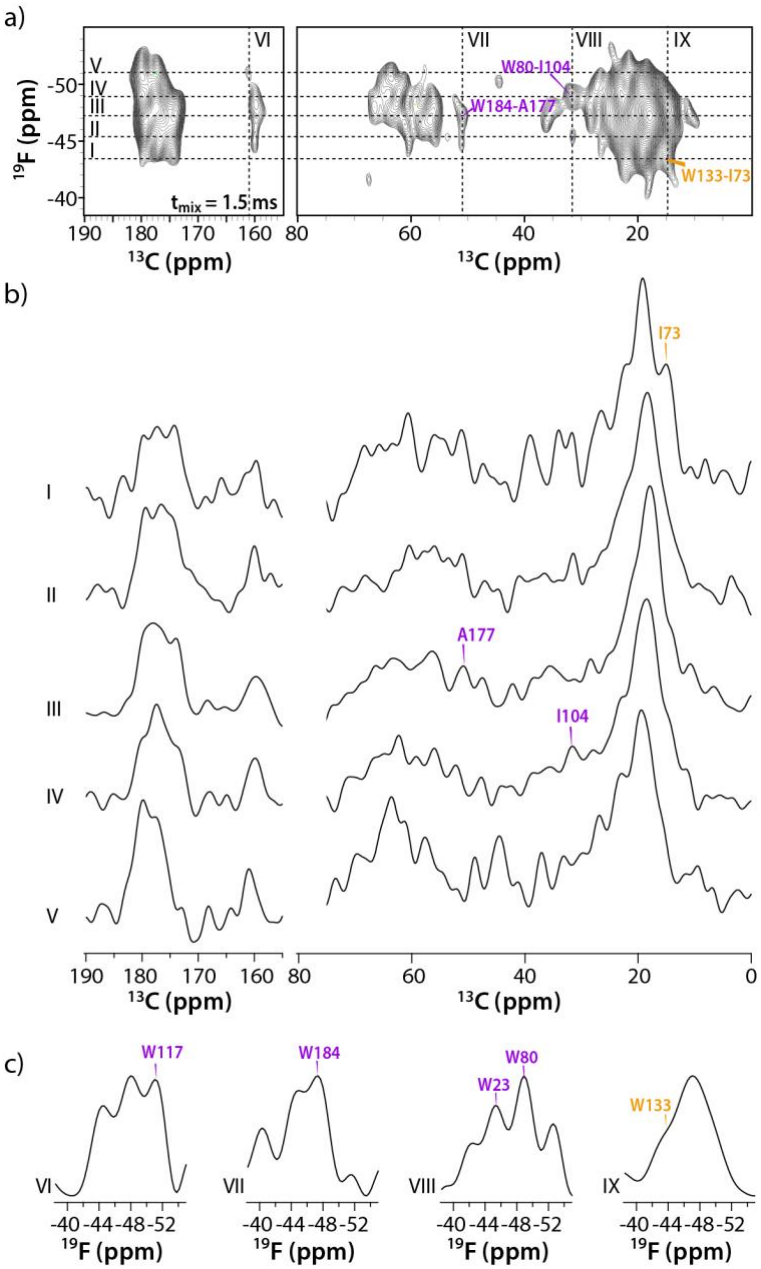

Figure S6. a) 2D ^{19}F-^{13}C DNP-enhanced HETCOR spectrum of 5F-Trp,U-^{13}C,^{15}N CA tubular assemblies. b-c) One-dimensional traces extracted from the spectrum. The spectrum was acquired at 14.1 T (564.8 MHz ^{19}F Larmor frequency) with a MAS frequency of 24 kHz. The mixing time was 1.5 ms. The contour levels are set to 3.5 X the noise.

Table S1. Chemical shift perturbations, peak intensity changes, and peak line widths in ^{13}C-^{13}C RFDR MAS NMR spectra of tubular assemblies of 5F-Trp, U-^{13}C,^{15}N CA in the presence of 12 mM AMUPol compared to the non-doped sample.

Residue	Weaker or missing	Stronger	Shift (backbone atom) > 0.3 ppm			Line width (Hz)		
			Peak	CSP 1	CSP 2	Peak	No AMUPol	12 mM AMUPol
Q9	CA-CB							
M10	CA-CB							
S16	CA-CB		CA-CB	0.3	0.1			
N21	CA-CB							
I37	CA-CB							
N57	CA-CB							
T58	CB-CO					CA-CG	100.6	104.4
L83	CA-CB		CA-CB	0.4	0.2			
H84			CA-CO	0.2	0.6	CA-CO	96.8	82.7
P85/P90	CA-CG							
H87	CA-CB		CA-CO	0.3	0.1			
G89			CA-CO	0.3	0.6			
P93			CA-CB	0.3	0.2			
M96			CA-CB	0.3	0.0	CA-CB	200.0	149.7
R100		CA-CB						
S102	CA-CB							
T107	CA-CB	CA-CG				CA-CG	77.6	137.8
T108	CA-CB	CA-CG	CA-CO	0.4	0.1	CA-CG	91.8	200.0
S109	CA-CB							
T110	CA-CB	CA-CG				CA-CG	89.7	200.0
T119	CA-CB	CA-CG						
H120			CA-CO	0.3	0.5	CA-CO	106.8	120.6
N121	CA-CB	CA-CO	CB-CO	0.1	0.3			
I124	CA-CB					CA-CG	132.0	72.2
I129			CA-CG1	0.4	0.2			
T148		CA-CB						
I153	CA-CB		CA-CB	0.4	0.4	CA-CB	99.6	118.6
E159	CA-CB							
F161			CA-CB	0.3	0.2	CA-CB	199.9	200.0
Y169			CB-CO	0.3	0.5			
E175		CA-CB						
A177		CA-CB				CA-CB	142.0	117.7
W184	CA-CB							
T188	CA-CB							

A204	CA-CB		CA-CB	0.3	0.1			
L205	CA-CG							
V221		CA-CG						
L231	CA-CB							

Table S2. Sensitivity of ^{19}F MAS NMR and DNP-enhanced MAS NMR experiments on 5F-Trp, U-^{13}C,^{15}N CA.

Sample	Sample amount (mg)	Field strength (T)	MAS frequency (kHz)	Temperature (K)	Microwave power (W)	Recycle delay (s)	SNR*	ASR**
5F-Trp, U-^{13}C,^{15}N CA	14.6	19.95	24	290	0	8	0.016	-
5F-Trp, U-^{13}C,^{15}N CA, 4.3 mM AMUPol	11.0	14.1	24	120	0	10	0.015	-
					13.8	4	0.200	12
						6	0.191	12
						8	0.195	12
						16	0.198	12
						64	0.146	9
5F-Trp, U-^{13}C,^{15}N CA, 22.8 mM AMUPol	11.7	14.1	24	120	0	10	0.007	-
					13.8	4	0.236	15
						6	0.391	24
						8	0.342	21
						16	0.296	18
						64	0.226	14
5F-Trp, U-^{13}C,^{15}N CA, 28.2 mM AMUPol	11.6	14.1	24	120	0	60	0.012	-
					13.8	4	0.475	29
						6	0.460	28
						8	0.408	25
						16	0.458	28
						64	0.355	22

*Signal-to-noise ratio, for the maximum-intensity peak, per unit of experiment time per mg of sample. No ^{1}H decoupling was used in any of the experiments.
**The absolute sensitivity ratio between the DNP-enhanced experiments at cryogenic temperatures and non-DNP experiments at 290 K acquired at optimum recycle delays range from 12 to 29, taking into account the dependence of the signal intensity on the magnetic field strength ($B_0^{3/2}$).

Table S3. Tentative assignments of correlations in the ^{19}F-^{13}C DNP-enhanced HETCOR spectrum.

Distance (Å)	Assignments	^{19}F (ppm)	^{13}C (ppm)	Appear tmix (ms)	Disappear tmix (ms)
6.0	W117F-P99CA	-51.4	62.5	0.5	5
6.1	W117F-T110CG2	-50.8	21.5	0.5	
7.5	W133F-T107CG2	-43.1	22.8	0.5	
7.9	W133F-V126CG1	-43.1	22.9	0.5	
7.8	W184F-I150C	-47.1	175.5	0.5	
6.6	W184F-I150CG2	-47.7	18.0	0.5	
7.0	W184F-L151CA	-47.1	56.6	0.5	
6.4	W184F-L151CD1	-47.3	23.8	0.5	
4.4	W184F-M185CB	-47.6	31.8	0.5	1.5
7.9	W184F-N183C	-47.1	175.4	0.5	
6.5	W184F-T188C	-47.1	174.5	0.5	
5.8	W184F-T188CG2	-47.1	21.9	0.5	
7.6	W184F-V181CB	-47.6	31.8	0.5	1.5
6.4	W184F-V181CG1	-47.4	23.8	0.5	
5.2	W23F-I37C	-45.3	176.1	0.5	
7.3	W23F-I37CG2	-45.3	18.5	0.5	
8.0	W23F-L43C	-45.3	176.1	0.5	
6.0	W23F-L43CG	-45.4	27.1	0.5	
5.7	W23F-M55CE	-45.5	16.0	0.5	
7.5	W23F-S41C	-45.3	176.1	0.5	
5.6	W23F-V26CG2	-45.6	22.4	0.5	
4.8	W23F-V36CG1	-45.6	22.5	0.5	
7.5	W80F-E79C	-48.7	178.2	0.5	
6.8	W80F-H84CA	-48.4	54.4	0.5	
7.4	W80F-I104CB	-47.4	35.6	0.5	2.5
5.2	W80F-I104CD1	-48.6	12.0	0.5	2.5
7.1	W80F-I104CG2	-47.7	18.0	0.5	
7.1	W80F-I129C	-48.7	178.3	0.5	
6.1	W80F-I129CA	-48.9	64.6	0.5	5
4.2	W80F-I129CG1	-48.5	26.6	0.5	
4.4	W80F-I129CG2	-47.7	18.0	0.5	
7.7	W80F-P125C	-48.7	178.2	0.5	
6.3	W80F-R132CZ	-48.2	159.6	0.5	

8.0	W80F-V126CA	-48.9	64.7	0.5	5
5.9	W80F-W80CA	-48.7	63.1	0.5	2.5
5.6	W80F-W80CB	-48.5	26.6	0.5	
6.7	W133F-I73CD1	-43.4	14.9	1.5	2.5
8.8	W184F-A177CA	-47.3	50.9	1.5	5
8.0	W184F-K182CA	-46.4	61.1	1.5	5
6.0	W184F-L189CA	-46.7	58.4	1.5	
4.3	W184F-M185CA	-46.7	58.4	1.5	
7.9	W184F-T186CA	-48.0	66.5	1.5	5
6.5	W184F-T188CA	-47.3	63.9	1.5	2.5
7.4	W184F-V181CA	-48.0	66.5	1.5	5
6.1	W184F-W184CA	-46.4	61.1	1.5	5
7.3	W23F-L43CA	-45.3	55.8	1.5	
6.5	W80F-I104CG1	-49.0	31.6	1.5	2.5
10.4	W133F-R100CZ	-44.1	160.4	2.5	
10.9	W133F-R132CZ	-44.1	160.4	2.5	
7.8	W184F-I150CB	-47.2	39.5	2.5	
8.7	W23F-A31CA	-45.9	53.7	2.5	5
8.2	W23F-A42CA	-45.9	53.7	2.5	5
7.7	W23F-L138CB	-45.6	41.4	2.5	
4.0	W23F-M39CB	-46.4	32.2	2.5	
7.6	W23F-M55CB	-46.4	32.2	2.5	
7.6	W23F-S41CB	-45.1	63.8	2.5	5
7.9	W23F-S44CB	-45.1	63.8	2.5	5
7.9	W23F-V24CA	-45.1	63.8	2.5	5
8.0	W117F-L111CB	-50.6	40.0	5	
9.5	W117F-M96CA	-50.5	56.1	5	
8.4	W117F-M96CG	-50.8	30.4	5	
8.2	W117F-R100CB	-50.8	30.4	5	
9.1	W117F-R97CA	-50.5	56.1	5	
8.7	W117F-R97CB	-50.8	30.4	5	
9.9	W133F-E75CG	-42.5	34.9	5	
9.7	W133F-E79CG	-42.5	34.9	5	
9.6	W133F-G127C	-42.0	174.7	5	
9.4	W184F-K182CB	-47.5	34.0	5	
9.1	W23F-K25CA	-44.8	60.4	5	
9.5	W23F-K30CA	-44.3	56.2	5	
8.6	W23F-M55CA	-44.8	60.4	5	

7.7	W23F-P38CG	-45.1	27.8	5
10.0	W80F-A78C	-48.3	182.3	5
10.6	W80F-E79CD	-48.3	182.3	5
10.0	W80F-E79CG	-48.0	35.5	5
11.9	W80F-E98CD	-48.3	182.3	5
9.8	W80F-Y130CB	-48.0	35.5	5

Table S4. ^{19}F-^{19}F distances in the hexamer structure of the HIV-1 CA protein.

PDB 4XFX* CA NL4-3

5-F-Trp-CA	W23	W80	W117	W133	W184
	Intramolecular Distance (Å)				
W23	20.0	23.1	23.4	19.1	28.6
W80	33.3	34.1	12.6	8.8	33.1
W117	25.1	21.7	28.5	9.8	42.5
W133	26.2	28.6	27.2	33.0	33.8
W184	33.0	35.8	32.2	27.6	2.1-9.4
F-F	Intermolecular Distance (Å)				

*F atoms were added at the 5 position of the indole ring of all tryptophans.